EXPERIMENTAL EVALUATION BY SONIC ANEMOMETRY OF AIR FLOW IN A MEDITERRANEAN GREENHOUSE EQUIPPED WITH A PAD-FAN REFRIGERATION SYSTEM

Journal:	*American Society of Agricultural and Biological Engineers*
Manuscript ID:	SE-08348-2009.R1
Journal Name:	Transactions of the ASABE
Manuscript Type:	Full-length article
Date Submitted by the Author:	
Complete List of Authors:	Valera, Diego; UNIVERSIDAD DE ALMERIA, INGENIERIA RURAL Lopez, Alejandro; Universidad de Almeria, Ingenieria rural Molina-Aiz, Francisco; Universidad de Almeria, Ingenieria rural Peña, Araceli; Universidad de Almeria, Ingenieria Rural
Keywords:	greenhouses, cooling systems, anemometers, temperature, fans, pad
Abstract:	The aim of the present work is to study the airflow and distribution of temperature and humidity in a multi-tunnel greenhouse equipped with a pad-fan refrigeration system. Maximum values of air velocity were recorded at the entrance of the pads. In the first meters of air inside the greenhouse, high levels of turbulence intensity were recorded, as the air dampened by the pads mixed with the hot, dry air inside and the air flow cross-section increased. The crop has a clear stabilizing effect on the airflow, producing lower energy levels and turbulence than when the greenhouse is empty. Major temperature gradients were observed both horizontally and vertically inside the greenhouse. The maximum temperature gradient was recorded in the greenhouse which was empty, with an increase between the entrance of air through the pad and the exit through the extractor fans of 5.2ºC. With a crop in the greenhouse, the maximum difference in temperature was 2.3ºC. Abstract.doc

THIS PAGE IS FOR INDEXING PURPOSES AND WILL NOT BE PRINTED.

Before using the template, make sure that Word's AutoFormat features are all off

(select AutoFormat from the pull-down Format menu).

Author(s)

First Name	Middle Name	Surname	Role	Type (Corresp)
Diego	L	Valera	ASABE Member Engineer, Professor.	Y

Affiliation

Organization	URL	Email
Department of Rural Engineering. University of Almería. Carretera de Sacramento, s/n. 04120 Almería, Spain. Phone: +34 950015546; fax: +34 950015491; e-mail: dvalera@ual.es	http://cms.ual.es/UAL/universidad/departamentos/ingenieriarural/personas/persona/index.htm?idTurcana=6376&id=505553504857554875	dvalera@ual.es

Author(s)

First Name	Middle Name	Surname	Role	Type (Corresp)
Alejandro		López	Lecturer	N

Affiliation

Organization	URL	Email
Department of Rural Engineering. University of Almería. Carretera de Sacramento, s/n. 04120 Almería, Spain.		alexlopez@ual.es

Author(s)

First Name	Middle Name	Surname	Role	Type (Corresp)
Francisco	D	Molina-Aiz	Associate Professor	N

Affiliation

Organization	URL	Email
Department of Rural Engineering. University of Almería. Carretera de Sacramento, s/n. 04120 Almería, Spain.		fmolina@ual.es

Author(s)

First Name	Middle Name	Surname	Role	Type (Corresp)
Araceli		Peña	Professor	N

Affiliation

Organization	URL	Email
Department of Rural Engineering. University of Almería. Carretera de Sacramento, s/n. 04120 Almería, Spain.		apfernan@ual.es

EXPERIMENTAL EVALUATION BY SONIC ANEMOMETRY OF AIR FLOW IN A MEDITERRANEAN GREENHOUSE EQUIPPED WITH A PAD-FAN COOLING SYSTEM

A. Lopez, D.L. Valera, F.D. Molina-Aiz, A. Peña

The authors are **Diego L. Valera, ASABE Member Engineer,** Professor, Alejandro López, Lecturer, Francisco D. Molina-Aiz, Associate Professor and Araceli Peña, Professor, Department of Rural Engineering, University of Almería, Spain. **Corresponding author:** Diego L. Valera, Department of Rural Engineering, University of Almería, Carretera de Sacramento s/n, 04120 Almería, Spain; phone: +34 950015546; fax: +34 950015491; e-mail: dvalera@ual.

Abstract. *The aim of the present work is to study the air flow and distribution of temperature and humidity in a multi-span greenhouse equipped with a pad-fan cooling system operating both with a well-developed tomato crop and without crop (simulating recently transplanted plants in the greenhouse). Maximum values of air velocity were recorded at the entrance of the pads. In the first meters of air inside the greenhouse, high levels of turbulence intensity were recorded, as the air dampened by the pads mixed with the hot, dry air inside and the air flow cross-section increased. The crop has a clear stabilizing effect on the air flow, producing lower energy levels and turbulence than when the greenhouse was empty. The maximum temperature gradient was recorded in the greenhouse which was empty, with an increase between the entrance of air through the pad and the exit through the extractor fans of 5.2 ºC. This climate heterogeneity when young plants are transplanted in the greenhouse can produce over-consumption of irrigation water, which must be considered by the growers to avoid plant damage by water stress. With a crop in the greenhouse, the maximum difference in temperature was reduced to 2.3 ºC.*

Keywords. *Greenhouses, cooling systems, fans, pad, anemometers, temperature.*

INTRODUCTION

The installation of evaporative cooling systems has increased over recent years in areas like southeast Spain, with a high concentration of greenhouses and high temperatures during spring-summer. Furthermore, these systems are not used solely to reduce temperature, but rather to maintain a suitable hygrometric regime. This climatic control technique is of particular interest when crops are transplanted and in the first developmental stages, when plants have little foliage and low evapotranspiration. Using this system in Almería (Spain), for example, the transplant date of some autumn-winter crops could be brought forward to the month of August, when temperatures are extremely high (Valera et al., 2008).

Temperatures in a commercial greenhouse equipped with a ventilated cooling–pad system and a half–shaded plastic roof were up to 10ºC cooler than outside (Kittas *et al*., 2001). Their main disadvantage was the thermal gradient generated in the direction of the air flow of up to 8 ºC (Kittas *et al*., 2003). By combining these systems with shading screens energy consumption was reduced by 8%, and air temperature rise along the greenhouse was reduced by 18% compared to an unshaded greenhouse (Willits and Peet, 2000).

Using the fan and pad system greater temperature drops are obtained (maximum values of 3.4 ºC compared to a naturally ventilated greenhouse) and fruit quality and size are improved in comparison with misting systems and natural ventilation (Willits and Li, 2005). The presence of the crop inside the greenhouse has a notable influence on the distribution of temperature and humidity brought about by the use of evaporative pads, as it reduces the vertical temperature gradient generated by the cooling system (Li and Willits, 2008).

The information compiled by Sethi and Sharma (2007) about the cooling technologies available worldwide for agricultural greenhouses (fan-pad, mist/fog and roof cooling) shows that fan-pad cooling is an effective method of lowering the air temperature of the greenhouse, as inside air temperature can be lowered between 4–6 ºC if used alone and 4–12 ºC if used along with shading. The main advantage of this method is that it does not entail any risk of wetting the foliage and the main disadvantage are the lack of uniformity of the climatic conditions, which are characterized by rising temperature and falling humidity along the length of the structure and in the air flow direction (Arbel *et al.*, 2003).

Sethi and Sharma (2007) concluded than none of the currently available technologies meets all the cooling requirements of the greenhouse and inside crops. The selection and operation of the system is based on various parameters such as type of climate, crop, cost, maintenance, ease of operation, reliability, life of the system, dependence on electricity, etc. Therefore, the most suitable technology for greenhouse cooling is that which meets most of the desired conditions of the farmer to grow off-season crops in order to make maximum profit.

Arbel *et al.* (2003) suggested that future studies be focused on characterization of the air flow in greenhouses equipped with pad-fan cooling. Measurement of air flow in real greenhouses has traditionally been carried out using tracer gas, by calculating the pressure difference between outside and inside the greenhouse (Wang and Deltour, 1997), or with velocity sensors (Boulard *et al*., 1996-1998; Boulard *et al*., 2000; Wang and Deltour, 1999). Air velocity can also be evaluated by sonic anemometry, measuring the influence that air velocity has on the transmission time of ultrasonic pulses between two pairs of transmitters-receptors (Cuerva and Sanz-Anders, 2000). This system allows instant air velocity values to be obtained for the three spatial axes. It also allows the average value to be separated from the turbulent flow component (Boulard *et al*., 1996).

The capacity to maintain homogeneous climatic conditions in greenhouses depends on the design and performance of the climatic control system. The air flow pattern relates the outdoor environment to the greenhouse microclimate and crops growing in greenhouses. By understanding the microclimate distribution growers can optimize fertilization and irrigation systems and improve factors linked to climate heterogeneity such as over-consumption of irrigation water or nitrogen loss to the environment (Boulard and Wang, 2002). Using sonic anemometry the greenhouse microclimate distribution generated by a pad cooling system can be described by measuring air temperature and velocity at several points. Moreover, sonic anemometry allows analysis of the air flow turbulence that enhances heat transfer, due to the increase of convective transport by turbulence that also results in mixing of substances and dispersal of momentum (Mathieu and Scott, 2000). An important characteristic of turbulence is its ability to transport and mix fluid much more effectively than a comparable laminar flow (Pope, 2009). Thus, a by-product of turbulence is the mixing of substances (Mathieu and Scott, 2000) such as water vapor, which directly influences the homogeneity of the greenhouse microclimate when cooling pads are used.

For the reasons explained above, sonic anemometry has been chosen as the ideal method for evaluating the air flow pattern and temperature distribution generated by forced ventilation. This measurement technique has allowed us to analyze how the air wetted in the pad mixes with the dry, warm inside air. Anemometric measurements have also allowed us to compare the level of turbulence in the air flow inside the greenhouse with measurements recorded in naturally ventilated greenhouses by other authors. In addition to the air velocity inside the greenhouse, the temperature and humidity produced by evaporative pad cooling systems have been measured in a vertical profile. In order to study the influence of the crop, measurements were taken inside the greenhouse with a well-developed tomato crop and when the greenhouse was empty (to simulate recently transplanted plants).

Material and Methods

Experimental Setup

The experimental work took place in a multi-span greenhouse located at the agricultural research farm belonging to the University of Almería, in south-eastern Spain (36º51' N, 2º16' W and 87 m elevation). The cropped soil had an artificial layer of sand mulch on the surface; these mulched soils are known locally as 'enarenado' (Wittwer and Castilla, 1995; Castilla and Hernández, 2005). The greenhouse, of 24×45 m (1080 m^2), was divided into two halves by a polyethylene sheet, which allows us to study the inside microclimate of the two halves separately for other research works. The two measurement tests (with and without crop) were carried out in the eastern half of the experimental greenhouse (Fig. 1), but with the cooling system operating in the whole greenhouse and with the crop growing in identical conditions in the two halves of the greenhouse. The first of the measurement tests (Fig. 2a) was carried out in the presence of a tomato crop, type 'Cherry' (*Solanum lycopersicum* L. cv. Salomee) with an average height of 2.2 m and a leaf area index of 1.69 $m^2\ m^{-2}$. The second test was carried out without crop (Fig. 2b), which is similar to the situation when little plants are transplanted into the greenhouse from the nursery. In these conditions the plants' evapotranspiration is negligible as it does not contribute to the cooling and the wetting of the inside air due to the crop's reduced leaf area. The aim of studying this system with the empty greenhouse was to analyze the possibility of advancing the transplant date to the beginning of August. In both measurement tests air flow was measured in four transversal sections of the greenhouse around the first extractor fan in the eastern sector (sections I-IV).

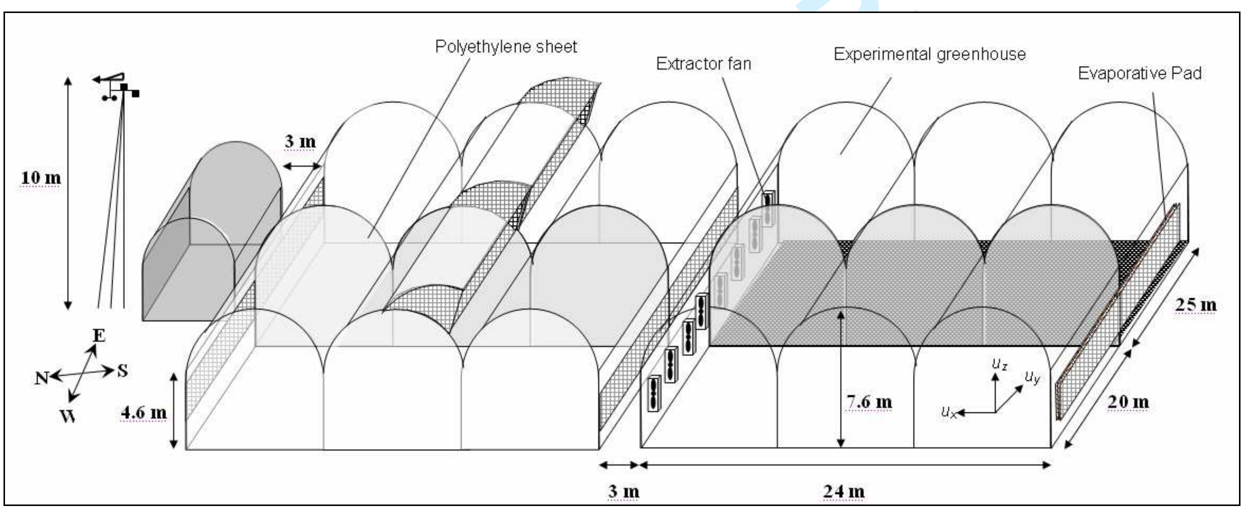

Figure 1. Diagram of the experimental greenhouse and the adjacent one.

Celdek® evaporative pads (Munters AB, Suecia) (2×40 m) were installed on the southern side, and eight extractor fans were placed on the northern side, four in each sector of the greenhouse. In order to prevent insects entering through the evaporative pads a 10×20 thread cm^{-2} insect-proof screen was placed on the outside [33.5% porosity, pore width 233.7 µm, pore height 724 µm, thread thickness 275 µm (Valera *et al.*, 2006)]. To the north the greenhouse is bordered by another multi-span greenhouse (Fig. 1), while to the south there are no obstacles.

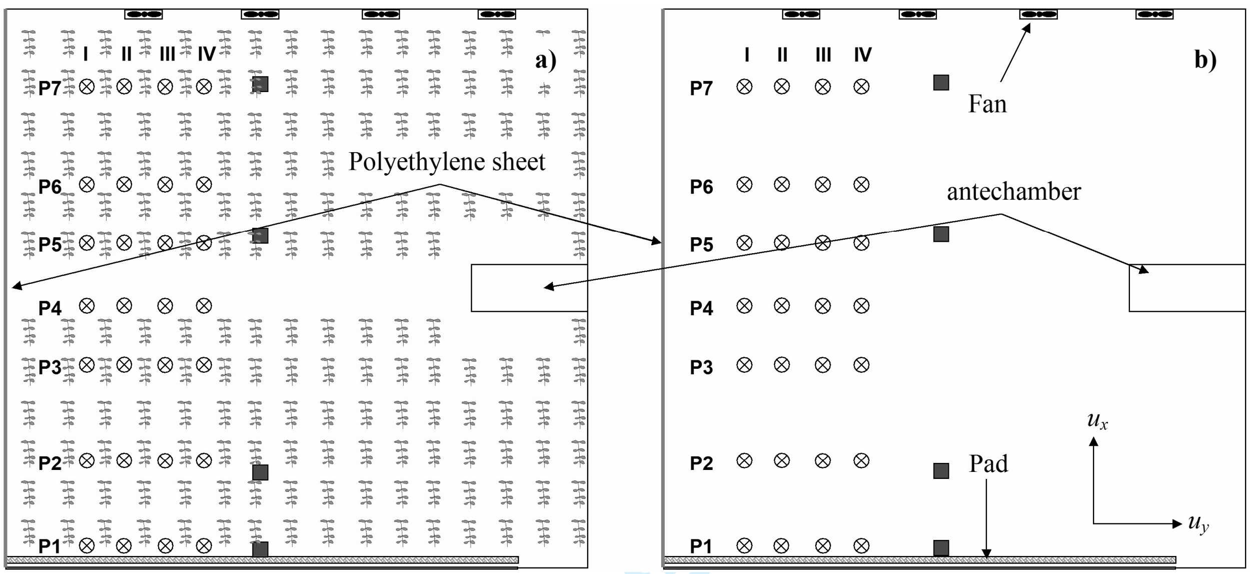

Figure 2. Distribution of the sensors for the measurement tests in the eastern sector of the greenhouse. ⊗ Measurement points with the sonic anemometer (CSAT3) and ■ location of the temperature and humidity sensors. Profiles between the crop rows for the measurement test on 22/7/2008 (a) and without crop on 11/08/2008 (b).

EQUIPMENT AND INSTRUMENTATION

Air velocity and temperature inside the greenhouse were measured with a 3D sonic anemometer (model CSAT3, Campbell Scientific Spain S.L., Spain; resolution: 0.001 m s^{-1} and 0.002 ºC; accuracy ±0.04 m s^{-1} and ±0.026 ºC; vertical path length: 5.8 cm, measurement rate: up to 60 Hz). Data were recorded by a CR3000 Micrologger (Campbell Scientific Spain S.L., Barcelona, Spain), with a data registration frequency of 10 Hz (Shilo *et al.*, 2004 and Molina-Aiz *et al.*, 2009). Figure 2 shows the location of the air flow and temperature measurements recorded in the eastern sector of the experimental greenhouse.

Outside climatic conditions were recorded by a meteorological station at a height of 10 m located to the north of the greenhouse (Fig. 1). The meteorological station included a BUTRON II (Hortimax S.L., Spain) measurement box with a Pt1000 temperature sensor and a capacitive humidity sensor, with a temperature measurement range of -25 ºC to 75 ºC and accuracy of ±0.01 ºC, and a humidity range of 0% to 100% and accuracy of ±3%. Outside wind speed was measured with the Meteostation II (Hortimax S.L., Spain), incorporating a cup anemometer with a measurement range of 0 – 40 m s^{-1}, accuracy of ±5% and a resolution of 0.01 m s^{-1}. Wind direction was measured with a vane (accuracy ±5º and resolution 1º). Solar radiation was measured using a Kipp Solari (Hortimax S.L., Spain) sensor, with a measurement range of 0 – 2000 W m^{-2}, accuracy of ±20 W m^{-2} and a resolution of 1 W m^{-2}.

Temperature and humidity inside the greenhouse were measured using 6 autonomous data-loggers HOBO® Pro Temp-HR U23-001 (Onset Computer Corp.) placed in a vertical profile under the ridge of the three greenhouse spans at heights of 1 and 2 m, while a seventh sensor was placed on the evaporative pad. These fixed devices allowed temperature measurement in a range of -40 ºC a 70 ºC with an accuracy of ±0.18 ºC and measurement of relative humidity of 0% to 100% with an accuracy of ±2.5%. They were all programmed to register data at 0.5 Hz, and were protected against direct solar radiation with a passive solar radiation open shield.

From the data of inside humidity recorded by the fixed sensors we can obtain the specific humidity ***q*** and correct the sonic anemometer temperature using the following expression (Tanny *et al*., 2008):

$$T_{sc} = \frac{T_s}{1 + 0.51q} \tag{1}$$

During the measurement tests, the EM50 extractor fans (Munters Europe AB, Sollentuna, Suecia) were working at 40 Hz, a theoretical flow of 5.6 m^3 s^{-1}, and the water flow over the surface of the pad was 3.3 l h^{-1} m^{-2}. The readings of air velocity were taken with the anemometer situated 1.5 m above the ground.

ANALYSES

Mean and turbulent air velocities

For air velocity $\boldsymbol{u}$ and its components [longitudinal $\boldsymbol{u_x}$, transversal $\boldsymbol{u_y}$ and vertical $\boldsymbol{u_z}$ (Fig. 1)], the mean air velocity measured over a period Δt is (Cebeci, 2004):

$$\bar{u} = \frac{1}{\Delta t}\int_t^{t+\Delta t} u\,dt \tag{2}$$

We have also calculated the average value of two-dimensional horizontal resultant of air velocity in *XY* (*l*) plane and two-dimensional vertical resultant of air velocity in *XZ* (*v*). The time interval Δt must be longer than any significant fluctuation and short enough for the transitory ‘real’-time effects not to affect the integration, and so its value was fixed at 5 minutes (Wang and Deltour, 1997 and 1999; Wang *et al*., 1999; Chung, 2002; Teitel *et al*., 2005). This time period is a compromise between a shorter one that may reduce accuracy and a longer one that may increase the overall difference with regard to outside microclimate parameters (Molina-Aiz *et al*., 2009). At each of the measurement points with the sonic anemometer we recorded data for 5 minutes at a sampling frequency of 10 Hz. Calculations were made for each of the one minute periods (600 data) and for the whole 5 minutes (3000 data), ensuring that the data were coherent over time.

In Equation (1), ***u(t)*** is the instantaneous air velocity which can be expressed as the sum of time-mean value $\bar{u}$ and a fluctuating component ***u'(t)*** (Cebeci, 2004).

$$u(t) = \bar{u} + u'(t) \tag{3}$$

An instantaneous velocity is the average velocity plus the difference of the reading from the mean value. Turbulence is the variance of ***u'***. The variance of an air velocity over a period of time Δt , is defined as (Heber *et al*., 1996; Cebeci, 2004):

$$\sigma^2 = \overline{u'^2} = \frac{1}{\Delta t}\int_t^{t+\Delta t} (u - \bar{u})^2 dt \tag{4}$$

Turbulence intensity ***i*** is standard deviation σ divided by mean local velocity $\bar{u}$, so (Cebeci, 2004):

$$i = \frac{\sqrt{\overline{u'^2}}}{\bar{u}} = \frac{\sigma}{\bar{u}} \tag{5}$$

Measures of turbulence scale

The regularity factor of a time series is the total number of mean crossings (or zero crossings if the mean is subtracted from the series) divided by the total number of peaks between mean crossings (Heber and Boon, 1993). The normalized autocorrelation function ***R(t)*** is the correlation between air velocities at a fixed position at two different instants ***t*** y $t+\delta_t$ (Heber *et al*., 1996 and Cebeci, 2004):

$$R(t) = \frac{\overline{u'(t) \cdot u'(t+\delta_t)}}{\sigma^2} \tag{6}$$

The function ***R(t)*** measures the persistence of a velocity wave within the whole time series. A random fluctuation would give a rapidly decreasing autocorrelation function while a regular oscillation would lead to a wave. Such variation might be associated with a physical phenomenon such as an eddy (Wang and Deltour, 1999).

As opposed to integrating ***R(t)*** to infinity, it can only be integrated to the first zero crossing t_0 to obtain t_{int} , the 'integral' time scale (Heber *et al*., 1996; Wang and Deltour, 1999):

$$t_{int} = \int_0^{t_0} R(t) \cdot dt \tag{7}$$

and L_i , the integral length scale , also called the macroscale (Hinze, 1975) or the average size of the largest eddies (Melikov *et al*., 1990; Wang and Deltour, 1999):

$$L_i = \bar{u} \cdot t_{int} \tag{8}$$

Integral length scales are a measure of the extent of the mass of air that moves as a unit (Hazawa *et al*., 1987). These eddies carry the major part of the turbulent energy and they are responsible for the main velocity fluctuations (Heber *et al*., 1996).

The discrete energy spectrum

According to the turbulence theory, the turbulent flow can be regarded as the superposition of eddies of different scales (Ouyang *et al*, 2006). The spectral density function between two random signals is defined as the Fourier transform of the correlation function, and gives the distribution of the mean square of the signal over frequency. The spectrum of energy density ***E(f)*** [$m^2 s^{-1}$] gives the relationship between the frequency of a signal and the energy of the corresponding eddies (Lay and Bragg, 1988). By representing the density of energy against the frequency in a logarithmic scale provides a clear description of the energetic level of the air flow.

According to the sampling theorem, a frequency signal ***f*** remains contained in its samples uniformly spaced at intervals of less than 1/2 ***f*** (Lathi, 1994). The discrete power spectrum density function ***E(f)*** is calculated by (Ouyang *et al*, 2006):

$$E(f) = \frac{2\Delta t}{N} \left| X(f) \right|^2 = \frac{2\Delta t}{N} X(f) X^*(f) \tag{9}$$

X(f) is the Fast Fourier Transfer (FFT) of sample data X(t) of instantaneous velocity, and X*(f) is conjugate complex number of X(f).

The turbulent flow consists of a mass of eddies of different scales. The average negative slope ($\boldsymbol{\beta}$ value) of logarithmic power spectrum curves (also called power spectrum exponent) is the main parameter used in the analysis of air flow. $\boldsymbol{\beta}$ value can reflect the energy distribution of eddies of different scales, and the larger the $\boldsymbol{\beta}$ value, the more turbulent energy distributes in the eddies of large scale. Its relationship with ***E(f)*** can be expressed as the following (Cebeci, 2004 and Ouyang *et al*., 2006):

$$E(f) \propto f^{-\beta} \tag{10}$$

A mechanically generated air flow is characterized by energy density spectra of low slope (Ouyang *et al*., 2006). The slope of the energy spectrum for air flows generated naturally at the ventilation surfaces usually corresponds to an isotropic distribution of turbulence, $\boldsymbol{\beta}$=5/3 (Stull, 1988). Boulard *et al*. (2000) and Tanny *et al*. (2006) reported a similar slope of the spectrum in an empty greenhouse and in a banana screenhouse, respectively. The level of the spectrum at low frequencies indicates the amount of turbulent kinetic energy in the flow. The region of the spectrum at high frequencies corresponds to the level of energy dissipation (Boulard *et al*., 2000).

Microscale of turbulence $\boldsymbol{\lambda}$ is a measure of the dimension of eddies which, at the same intensity, produce the same dissipation as the turbulence considered (Panofsky and Dutton, 1984). Melikov *et al.* (1990) defined microscale as the average size of the smallest eddies mainly responsible for dissipation, and it can be calculated as (Hinze, 1975; Melikov *et al*., 1990):

$$\lambda = \left| \frac{\bar{u}^2 \sigma^2}{2\pi \int_0^\infty f^2 E(f) df} \right|^{\frac{1}{2}} \tag{11}$$

Total turbulence kinetic energy $\boldsymbol{k}$ [$m^2\ s^{-2}$] can be calculated by the following expression (Loomans, 1998; Easom, 2000):

$$k = \frac{1}{2}(\sigma_x^2 + \sigma_y^2 + \sigma_z^2) \tag{12}$$

where $\boldsymbol{\sigma_x}$, $\boldsymbol{\sigma_y}$ and $\boldsymbol{\sigma_z}$ are the standard deviations of the three air velocity components. The turbulence energy dissipation rate $\boldsymbol{\varepsilon}$ [$m^2\ s^{-3}$] is defined as (Heber *et al*., 1996):

$$\varepsilon = k^{3/2} \lambda^{-1} \tag{13}$$

Measure of cooling efficiency

The efficiency of a cooling system $\boldsymbol{\eta}$ can be defined as (ASHRAE, 1983):

$$\eta = \frac{T_{bs} - T_{cbs}}{T_{bs} - T_{bh}} \tag{14}$$

where, $\boldsymbol{T_{bs}}$ is the dry bulb temperature of the outside air, $\boldsymbol{T_{cbs}}$ is the dry bulb temperature of the cold air leaving the evaporative pads and $\boldsymbol{T_{bh}}$ is the wet bulb temperature of the outside air.

RESULTS AND DISCUSSION

The measurement tests were carried out under prevailing '*Levante*' (Northeast, NE) and '*Poniente*' (Southwest, SW) winds, the most usual ones in the province of Almería (Capel, 1990). The outside climatic conditions remained relatively stable over the two measurement tests (Table 1).

Table 1. Outside climatic conditions for the measurement tests: $\bar{u}_{ext}$, average wind speed; *D*, wind direction; HR_e, outside relative humidity; T_e, outside temperature.

Date	22/07/08			11/08/08		
Time	11:15-14:10			11:05-13:52		
	Mean±desv.est	max	min	Mean±desv.est	max	min
$\bar{u}_{ext}$, **m s^{-1}**	4.92±1.43	7.00	0.51	5.45±0.49	6.25	4.58
***D*, º**	72±21 (NE)	89	38	189±5 (SW)	198	181
HR_e, **%**	53±4	61	48	65±2	70	60
T_e, **ºC**	29.9±0.8	30.7	28.3	28.6±0.5	29.9	27.8
***Radiation*, W m^{-2}**	798.0±74.1	879.0	640.0	807.0±135.3	1045.6	400.8

AIR VELOCITY

The values of air velocity measured in the four transversal sections show that the principal component of air flow is $\boldsymbol{u_x}$, perpendicular to the evaporative pads, accounting for 85.7% and 84.5%, of the air velocity $\boldsymbol{u}$ (calculated as the average of the $\boldsymbol{u_x/u}$ ratio for the measurement points inside the greenhouse), for the measurements with and without plants, respectively (Tables 2 and 3). The average values of the longitudinal component $\boldsymbol{u_x}$ and the air velocity $\boldsymbol{u}$ were very similar. While the transversal and vertical components, $\boldsymbol{u_y}$ and $\boldsymbol{u_z}$, were less influential in the flow generated by the extractor fans.

Table 2. Average values of the air velocity and the three air velocity components, for the measurements on 22/07/2008, for the different sections and points (P) analyzed.

	P	***u*. m s^{-1}**	u_x**. m s^{-1}**	u_y**. m s^{-1}**	u_z**. m s^{-1}**
Section I	**1**	0.50±0.04	0.46±0.03	0.05±0.02	-0.19±0.03
	2	0.16±0.08	0.14±0.09	-0.08±0.08	0.07±0.07
	3	0.17±0.06	0.16±0.06	-0.02±0.07	0.07±0.05
	4	0.15±0.07	0.15±0.07	-0.02±0.07	0.02±0.06
	5	0.18±0.05	0.17±0.05	0.04±0.07	-0.01±0.04
	6	0.17±0.05	0.17±0.05	0.04±0.05	-0.14±0.05
	7	0.34±0.09	0.30±0.09	0.12±0.06	-0.06±0.07
Section II	**1**	0.75±0.06	0.70±0.05	0.07±0.03	-0.26±0.02
	2	0.41±0.11	0.39±0.12	-0.11±0.09	-0.03±0.09
	3	0.31±0.08	0.30±0.08	0.00±0.08	-0.03±0.07
	4	0.30±0.09	0.29±0.08	0.05±0.09	-0.03±0.05
	5	0.28±0.07	0.27±0.07	0.04±0.07	0.00±0.05
	6	0.34±0.06	0.31±0.06	0.06±0.06	-0.02±0.05
	7	0.22±0.07	0.16±0.07	0.13±0.05	-0.12±0.06
Section III	**1**	0.55±0.05	0.51±0.04	0.07±0.04	-0.19±0.02
	2	0.20±0.08	0.20±0.08	-0.03±0.08	-0.03±0.06
	3	0.13±0.05	0.13±0.05	0.00±0.05	0.01±0.06
	4	0.13±0.06	0.13±0.06	0.01±0.06	0.00±0.06
	5	0.18±0.04	0.17±0.04	0.05±0.05	0.00±0.05

	6	0.14±0.04	0.12±0.05	0.07±0.04	0.01±0.04
	7	0.31±0.09	0.26±0.07	0.15±0.06	-0.08±0.08
Section IV	**1**	0.66±0.06	0.61±0.07	0.07±0.03	-0.24±0.04
	2	0.25±0.07	0.24±0.07	0.02±0.07	-0.05±0.07
	3	0.18±0.05	0.18±0.05	0.00±0.05	-0.01±0.06
	4	0.21±0.07	0.19±0.06	0.03±0.06	-0.06±0.07
	5	0.22±0.05	0.21±0.05	0.07±0.05	0.00±0.06
	6	0.21±0.06	0.19±0.05	0.10±0.05	-0.04±0.06
	7	0.27±0.06	0.22±0.07	0.15±0.07	-0.04±0.06

Table 3. Average values of the air velocity and the three air velocity components, for the measurements on 11/08/2008, for the different sections and points (P) analyzed.

	P	***u*. m s^{-1}**	***u$_x$*. m s^{-1}**	***u$_y$*. m s^{-1}**	***u$_z$*. m s^{-1}**
Section I	**1**	0.51±0.05	0.48±0.06	0.05±0.03	-0.19±0.03
	2	0.26±0.10	0.26±0.10	-0.01±0.10	0.02±0.06
	3	0.34±0.10	0.33±0.09	-0.08±0.09	0.01±0.07
	4	0.38±0.11	0.38±0.10	-0.07±0.09	0.00±0.07
	5	0.36±0.08	0.36±0.08	-0.01±0.09	-0.04±0.06
	6	0.25±0.07	0.24±0.07	0.00±0.07	-0.03±0.06
	7	0.26±0.10	0.23±0.13	0.13±0.10	-0.03±0.08
Section II	**1**	0.58±0.07	0.55±0.07	0.05±0.02	-0.19±0.02
	2	0.11±0.10	0.10±0.13	0.01±0.11	-0.02±0.07
	3	0.23±0.08	0.23±0.08	-0.01±0.08	0.01±0.06
	4	0.32±0.09	0.32±0.09	0.02±0.09	0.02±0.07
	5	0.31±0.08	0.31±0.08	0.02±0.09	-0.04±0.08
	6	0.29±0.08	0.29±0.07	0.05±0.08	0.00±0.08
	7	0.37±0.09	0.33±0.11	0.16±0.10	0.03±0.09
Section III	**1**	0.48±0.10	0.44±0.10	0.06±0.04	-0.17±0.05
	2	0.10±0.07	0.09±0.09	-0.03±0.07	0.00±0.06
	3	0.16±0.07	0.16±0.07	0.03±0.07	0.02±0.06
	4	0.30±0.11	0.29±0.10	0.07±0.08	0.02±0.08
	5	0.47±0.11	0.44±0.11	0.16±0.08	-0.04±0.09
	6	0.36±0.14	0.34±0.15	0.11±0.09	-0.05±0.08
	7	0.40±0.10	0.36±0.12	0.17±0.09	-0.04±0.08
Section IV	**1**	0.52±0.07	0.46±0.07	0.06±0.04	-0.23±0.03
	2	0.10±0.06	0.04±0.08	-0.09±0.07	-0.02±0.06
	3	0.14±0.08	0.13±0.08	-0.02±0.07	-0.01±0.06
	4	0.19±0.07	0.19±0.07	0.00±0.08	-0.02±0.05
	5	0.31±0.09	0.29±0.08	0.10±0.08	-0.05±0.07
	6	0.34±0.14	0.31±0.15	0.14±0.09	-0.03±0.06
	7	0.36±0.12	0.31±0.13	0.17±0.09	-0.02±0.07

The temporal stability of the air flow can be indicated by the standard deviation of the velocity $\boldsymbol{\sigma}$, which remained constantly low in the presence of the crop, as is usual in air flow through porous media (Molina *et al.*, 2006). Table 2 shows that the zone of greatest temporal uniformity of air flow was the one closest to the evaporative pad (*Points* 7). At these points in the four sections analyzed the standard deviation values were very low, which indicates that the velocity during the whole measurement time (5 min) was close to the mean value (Fig. 3).

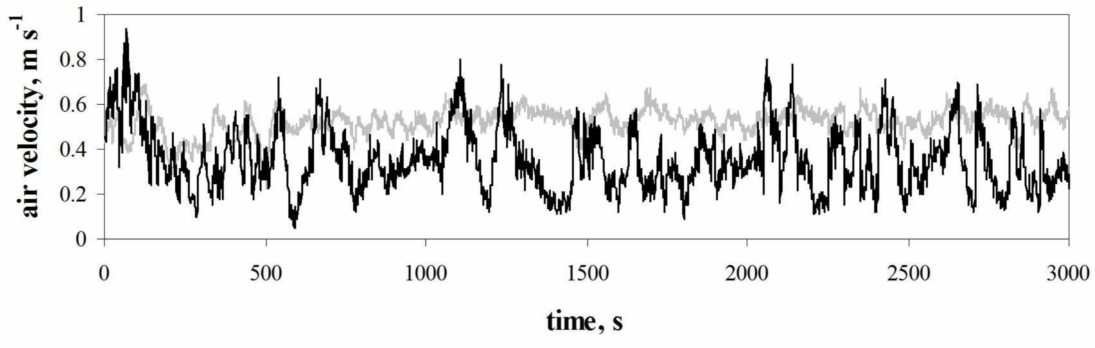

Figure 3. Recorded values of air velocity over 5 minutes for the measurement test on 11/08/2008: *Point P1-Section I* (gray line), *point P6-Section IV* (black line).

In the figure 4 we can observe the air velocity in the four sections analyzed for the two measurement tests. The spatial uniformity of air flow was also greater in the zone closed to the cooling pad (*Points 1*), where the air velocity maintained similar levels in the four sections analyzed, than in the other points (*Points 2 to 7*) for the empty greenhouse (Fig. 4b).

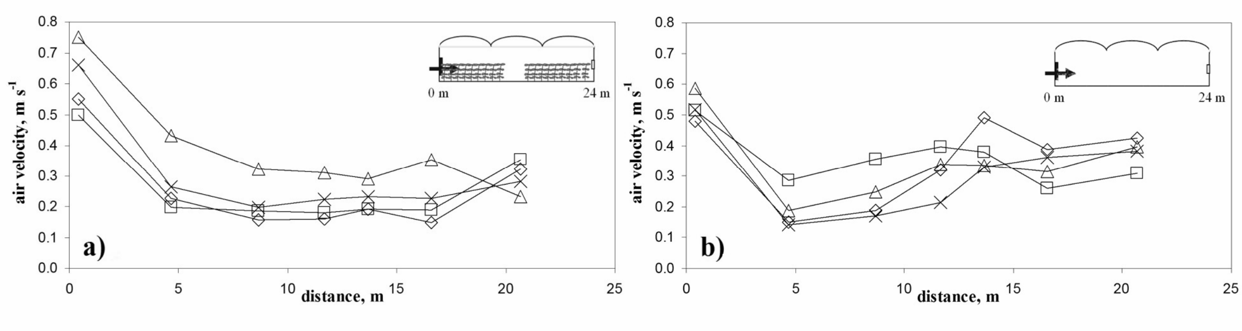

Figure 4. Profiles of absolute velocity corresponding to the measurements on 22/07/08 with crop (a) and on 11/08/2008 without crop (b): (-□-)section I; (-Δ-)section II; (-◊-)section III; (-×-)section IV.

In the presence of the crop, the air velocity in the different sections varied according to the distance between the crop lines. In the narrowest aisle (aisle *II* with a width of 0.6 m) the velocity close to the pad was greater than in the other aisles, while the minimum velocity at the pad was registered in aisle *I*, with a width of 1 m (Fig. 4a).

However, in the empty greenhouse the standard deviation increased, remaining higher than the average value for the horizontal component $\boldsymbol{u_x}$ at *points 2* in sections *II*, *III* and *IV* in the measurement test on 11/08/2008.

The vertical component $\boldsymbol{u}_z$ was very low at all points, except in the entrance section, where the air flow is downward. The transversal component $\boldsymbol{u}_y$ gains importance at the points closest to the extractor fans and to the pad where the air enters the greenhouse (Tables 2 and 3).

The air flow generated through the crop lines (Fig. 4a) maintained a light and more spatial uniform velocity than in the empty greenhouse (Fig. 4b). The average value for the horizontal component $\boldsymbol{u}_x$ inside the greenhouse, calculated as the mean of the average values at all *Points 2 - 7* (*Points* 1 closest to the pad were not considered), was 0.21±0.07 m s^{-1} with crop and 0.26±0.10 m s^{-1} without crop. In both cases, the current of damp air which passes over the surface of the evaporative pads, on coming into contact with the dry, warm air inside, and on increasing the air flow cross-section inside the greenhouse, undergoes a sharp drop in velocity (Fig. 4). In this case the minimum velocity is reached in the first span where the air enters the greenhouse, after which a positive velocity gradient develops until the exit of the air through the fans.

From the values of average velocity of the air entering the greenhouse through the pad, the pad's surface area and the volume of the greenhouse, the following renovation rates were obtained: 27.1 h^{-1} and 21.0 h^{-1} for the measurements on 22/07/2008 with crop and on 11/08/2008 without crop, respectively. Sethi and Sharma (2007) observed that a volume flow rate equivalent to 20 h^{-1} through the evaporative pads is sufficient to reach tolerable conditions inside the greenhouse under dry weather conditions.

In the test with crop, in which the velocity was measured in the aisles between the crop rows, there may have been a slight error, as at these points the velocity is somewhat greater due to the channeling of the air flow. The crop rows run from one end of the greenhouse to the other, coming into contact with the pads, and so measurements could only be taken in the aisles. These values are below the 35 to 90 h^{-1} recommended for greenhouses (ANSI/ASAE, 2003) and the optimum value of 45-60 h^{-1} (Hellickson and Walker, 1983; ANSI/ASAE, 1994). Nevertheless, this system improves considerably the number of renovations compared to the values observed with natural ventilation in the province of Almería, 5-15 h^{-1}, observed in Almería-type greenhouses (Molina-Aiz *et al*., 2009) and in Mediterranean greenhouses (Valera *et al*., 2009).

AIR FLOW DIRECTION

As well as obtaining the values of velocity for the different components, the air flow direction inside the greenhouse has been studied. Figure 5 shows the two-dimensional resultants of air velocity on the *XZ* plane ($\boldsymbol{v}$) and the frequency histograms of velocity directions (depicted as polar plots), allowing us to visualize the fluctuations in air direction on the vertical plane *XZ*.

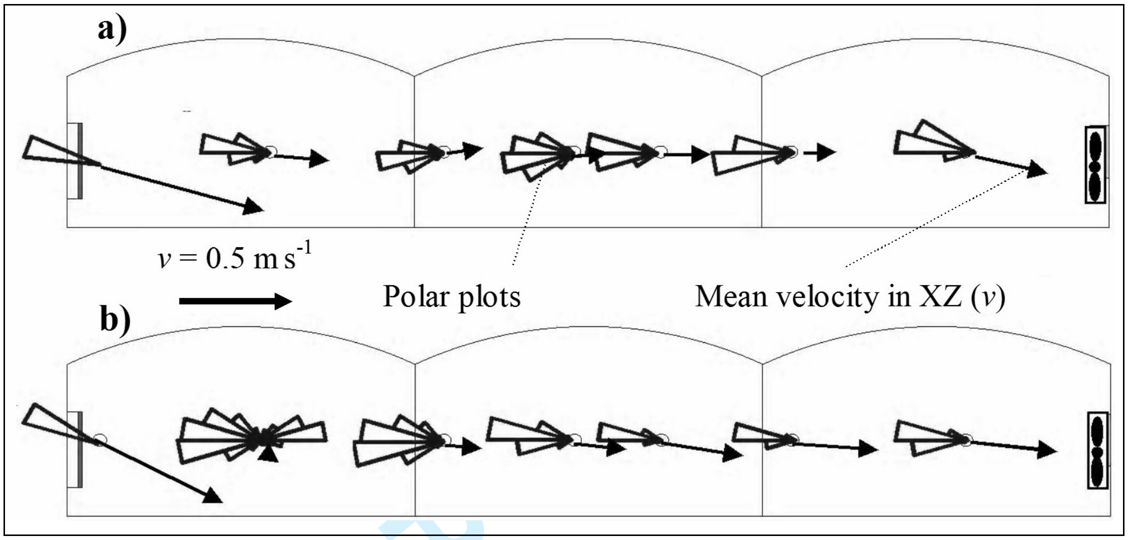

Figure 5. Two-dimensional resultants of air velocity on the *XZ* plane (*v*) and polar plots of air flow direction in the vertical plane *XZ* in the measurement test with crop on 22/07/2008 for section III (a) and without crop on 11/08/2008 for section IV (b).

When there is no crop, there is an increase in fluctuation in the direction of the air in the first span, giving rise to flows which run in the opposite direction to the main one (Fig. 5b). This greater fluctuation of air direction shows that when no crop was in the greenhouse, air flowed in different directions during measurements (5 minutes), including reverse flow for some moments. These changes in air direction may result from the convergence of moist cooled air from the pad with the drier, warmer air inside the greenhouse. Interaction between air masses with different density (temperature and/or moisture) characteristics can cause an increase in air flow turbulence, and consequently these fluctuations in air direction. When a crop was inside the greenhouse the difference between humidity of the air leaving the pad and air between the plants was lower (see Section *INTERIOR MICROCLIMATE*), reducing air fluctuations.

The flow of air entering through the pad has a downward sense, favoring the exchange of air in the lowest part of the crop (Fig. 5a), which does not always occur in conditions of natural ventilation, where the air currents which enter through the side windows are mainly horizontal (Valera *et al*., 2009).

Figure 6 shows the two-dimensional horizontal resultants of air velocity in the horizontal plane *XY* (***l***) and the frequency histograms of velocity directions.

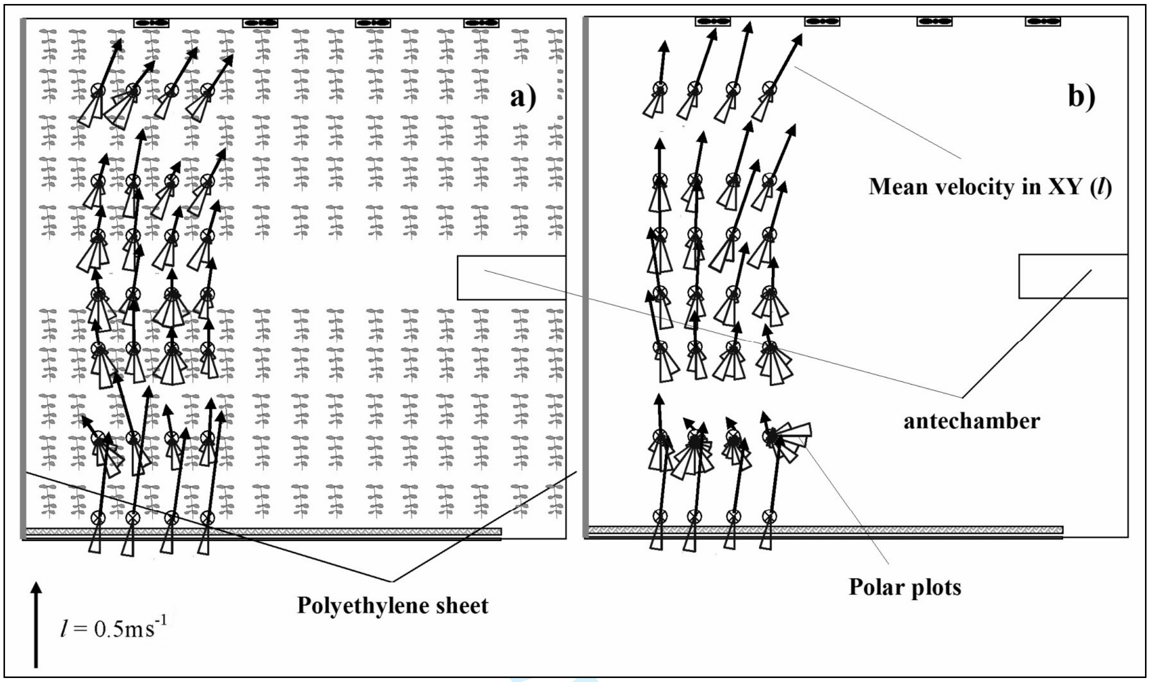

Figure 6. Two-dimensional resultants of air velocity on the *XZ* plane (*l*) and polar plots of air flow direction in the horizontal plane *XY* in the measurement test with crop on 22/07/2008 (a) and without crop on 11/08/2008 (b).

Overall, the mean air flow patterns measured for the two tests show that air flows perpendicular to the plane of the extractor fans and pad (Fig. 6). In the presence of the crop (Fig. 6a), the frequency histograms of velocity directions show less fluctuation of air direction in the first span closest to the pad (*Points 2*) than when the greenhouse was empty (Fig. 6b). As commented above, in the empty greenhouse there were more differences between characteristics (temperature and moisture) of the air masses inside and entering the greenhouse that contributed to air flow fluctuations. Moreover, when there was a crop inside the greenhouse, the air had to flow between the crop rows, and this may contribute to reducing the air direction fluctuation at *Points 2*.

TURBULENCE FLOW CHARACTERISTICS

Generally, the levels of turbulence (turbulence intensity, kinetic turbulent energy and its dissipation rate) measured inside the experimental greenhouse operating with a fan-pad cooling system were lower than the values observed in naturally ventilated greenhouses reported in the literature, see below. This lower turbulence of the cooling air flow reduces the mixing of the inside air with the outside air entering the greenhouse through the pad. Air turbulence is a characteristic of natural ventilation air flows which tends to homogenize the inside microclimate.

Turbulence intensity

Figure 7 shows the profiles of turbulence intensity obtained for the different points corresponding to the 4 sections of measurement for the two tests carried out with and without crop.

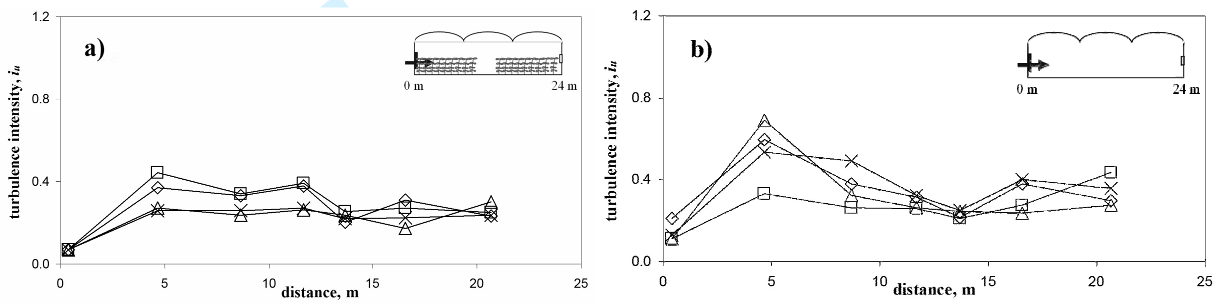

Figure 7. Profiles of turbulence intensity of the absolute velocity i_u corresponding to the measurement tests on 22/07/08 with crop (a) and on 11/08/2008 without crop (b): (-□-)section I; (-Δ-)section II; (-◊-)section III; (-×-)section IV.

In the previous section we have observed in which areas the air flow is most stable over time. The lowest levels of turbulence were recorded at the exit of the evaporative pads, measured at a distance of 40 cm from the pad. This may be due to the fact that the air has to pass through the porous media, the anti-insect screen and the evaporative pad, which produces the stabilizing effect on the air flow (Fang, 1997 and Fang *et al.*, 2001). Moreover, the forced currents at constant velocity are characterized by lower energy levels when compared to natural currents (Ouyang *et al.*, 2006).

On the inside of the greenhouse the levels of turbulence increase due to the greater mixture of air and the increase in the transversal air flow. Therefore, as the air circulates around the greenhouse, the turbulence intensity increases, reaching its maximum value 4.7 meters from the cooling pad (Fig. 7). This maximum value is lower when there is a crop in the greenhouse i_u=0.44 (Fig 7a), than when it is empty i_u=0.69 (Fig. 7b). From these maximum values, turbulence intensity falls steadily along the transversal section of the greenhouse (Fig. 7). Minimum values of turbulence intensity were recorded in the northern area of the greenhouse just before the air exits through the extractor fans (*Points 7*), and in the southern area just after the air passes through the evaporative pads (*Points 1*).

When there was no crop in the greenhouse, a greater increase was observed in turbulence intensity (Fig. 7) at the entrance of the greenhouse. The air flow entering through the pads shows little turbulence, becoming more turbulent inside the greenhouse before losing turbulence at the points closest to the extractor fans. The air flow was less uniform and more turbulent when there was no crop.

The levels of turbulence recorded at the entrance of the greenhouse through the pads with mechanical ventilation, ranging from 0.1 to 0.2, are lower than those reported for greenhouse windows by different authors in conditions of natural ventilation, ranging from 0.3 to 7.7 (Teitel *et al*., 2008; Valera *et al*., 2009; Molina-Aiz *et al*., 2009).

Boulard *et al*. (2000) observed that turbulence levels were lowest in the interior of the greenhouse and they increased at the windows. In the interior of the greenhouse, and with ventilation, Wang and Deltour (1999) and Tanny *et al*. (2006) recorded average values of turbulence intensity of i_x=0.80. In the present work, with mechanical ventilation the average turbulence intensity in the interior of the greenhouse with a crop was i_x=0.28 (22/07/2008), whereas without a crop it was i_x=0.35 (11/08/2008).

Measures of turbulence macroscale

In Figure 8 we can observe the values of the turbulent integral length scale or macroscale for the 4 measurement sections of the test without crop.

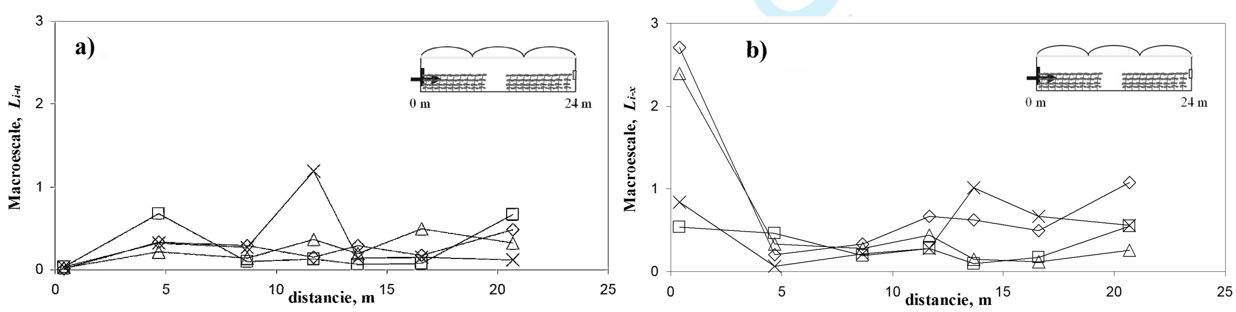

Figure 8. Profiles of air velocity macroscale L_{i-u} (a) and of macroscale for the horizontal direction L_{i-x} (b) and corresponding to the measurement test without crop on 11/08/2008: (-□-) section I; (-Δ-) section II; (-◊-) section III; (-x-) section IV.

The passage of air through the porous media, first the insect-proof screen and then the evaporative pad, produces stabilization of the air flow, giving rise to a greater dimension of the eddies for the horizontal component of the air

$L_{i\text{-}x}$ (1.23 and 1.65 m, mean value obtained for *Points 1* for tests with and without crop), i.e. perpendicular to the evaporative pads. On the other hand, for the air flow $L_{i\text{-}u}$ (0.00 and 0.02 m) and for the transversal and vertical components, $L_{i\text{-}y}$ (0.00 and 0.01 m) and $L_{i\text{-}z}$ (0.01 and 0.05 m), the value of the macroscale was very low.

In the interior of the greenhouse, the increases of transversal velocity and in turbulence intensity of the air flow give rise to a reduction in the macroscale (mean value of *Points 2 to 7*) in the main direction of the flow $L_{i\text{-}x}$ (0.04 and 0.06 m for the tests with and without crop). Inside the greenhouse the macroscale levels for the transversal $L_{i\text{-}y}$ (0.01 and 0.02 m) and vertical $L_{i\text{-}z}$ (0.01 and 0.06 m) components were also low, showing that the horizontal component was still the main one. Boulard *et al.* (2000) observed that the macroscale $L_{i\text{-}u}$ was maximum at the ventilation surfaces ($L_{i\text{-}u}$=8.3 m) and it fell towards the interior of the greenhouse, which did not have insect-proof screens. Wang and Deltour (1999) recorded values of the macroscale in the interior of a greenhouse with normal ventilation of $L_{i\text{-}x}$=11.9 m for the main direction of the flow and $L_{i\text{-}y}$=16.9 m for the transversal direction.

The discrete energy spectrum

In the **measurement test** without crop carried out on 13/08/2008 the slope of the spectrum was lower at the exit of the evaporative pad (β=0.76) than in the interior of the greenhouse, with values close to β=5/3. Low values of β are characteristic of mechanical air flows, in which the air is distributed uniformly between the range of frequencies considered (0-5 Hz) (Ouyang *et al.* 2006). At high frequencies, in the region of energy dissipation (Boulard *et al.*, 2000), the transport of energy is greater than with natural air flows in which energy is transported at low frequency (Ouyang *et al.* 2006). Figure 9 shows that in this test the fall of the spectrum at the points close to the evaporative pads was less abrupt than the average of the fall at the points in the interior.

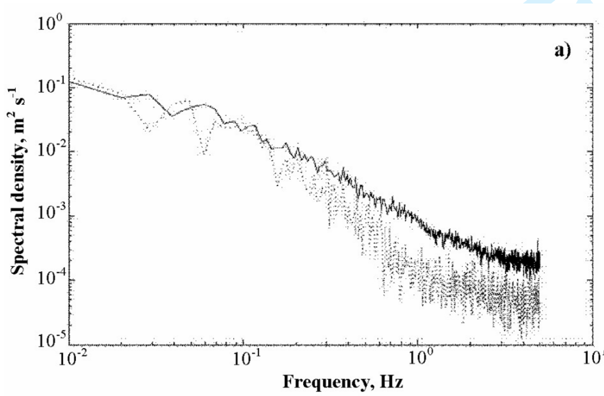

Figure 9. Average Energy density spectra at the evaporative pads (dotted line) and in the interior of the greenhouse (continuous line) for the measurement test on 11/08/2008.

The air flow coming out of the evaporative pads presents an average value of fall in the energy spectrum of $\boldsymbol{\beta}$=1.32 in the measurement test on 11/08/2008, respectively. Ouyang *et al*. (2006) established the characteristic value for air flows generated as $\boldsymbol{\beta}$=0.5 with centrifugal fans and $\boldsymbol{\beta}$=0.75 with axial fans (both for a velocity of $\boldsymbol{u}$= 0.25 ms^{-1}). In the interior of the greenhouse the values of the average slope of the energy spectrum were $\boldsymbol{\beta}$=1.10 and 1.23 for the two measurement tests (Table 4), i.e. lower than those of 1.5 to 1.7 obtained with natural ventilation (Boulard *et al*., 2000; Tanny *et al*., 2006 and Ouyang *et al*., 2006).

When there is a crop, there appears to be a reduction in the slope of the spectrum at the points in the centre of the greenhouse (Table 4). This reduction is sharper in the narrower aisles, where the air flow channeled by the crop rows causes a reduction in turbulence. On the other hand, in the empty greenhouse the levels of turbulence intensity and and the fall in the spectrum were greater, as is expected with natural ventilation flows.

Table 4. Average values of the slope of the spectrum at the exit of the pad ($\boldsymbol{\beta_p}$) and in the interior of the greenhouse ($\boldsymbol{\beta_i}$).

Date	$\boldsymbol{\beta_p}$	$\boldsymbol{\beta_i}$	$\boldsymbol{\beta_{i-max}}$	$\boldsymbol{\beta_{i-min}}$
22/07/2008	-	1.08	1.36	0.74
11/08/2008	1.37	1.24	1.61	0.78

Comparison of the energy density spectrum of the air flow at the outlet of the pads and in the interior of the greenhouse shows that the flow is more energetic and turbulent in the latter (the spectrum is greater). The region of energy dissipation at high frequencies indicates that more energy is dissipated in the centre of the greenhouse than at the pads (Fig. 9).

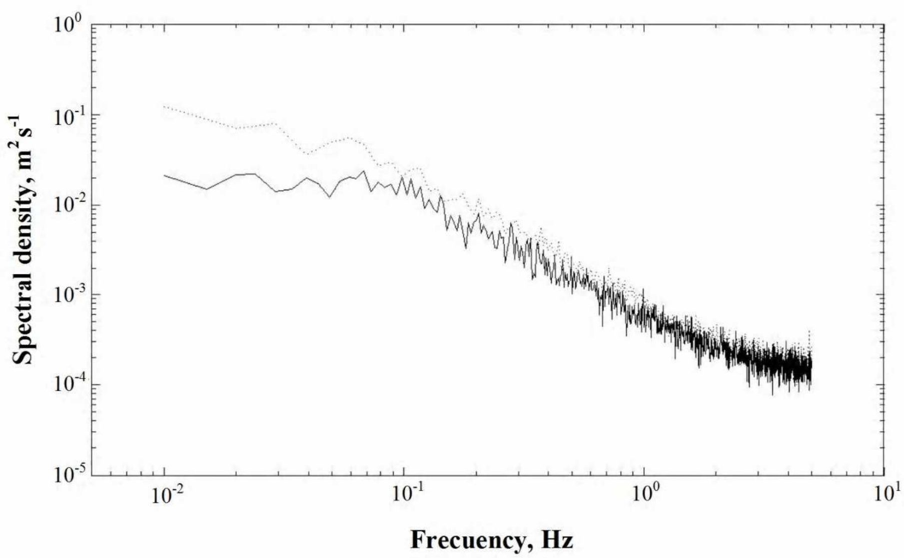

Figure 10. Average spectral density in the interior of the greenhouse for the measurement test with crop on 22/07/2008 (continuous line) and without crop on 11/08/2008 (discontinuous line).

Figure 10 shows that the air flow is less energetic with the crop (the spectrum was lower at low frequencies) due to the lower levels of turbulence, as was already observed for the turbulence intensity (Fig. 7a), and as we can also observe from the turbulent kinetic energy (Table 5). The spectral density for the two tests (with and without crop) does not present a clear difference at high frequencies in the region of energy dissipation.

Table 5. Average values of the turbulent kinetic energy ($m^2 s^{-2}$) at the exit of the pad (k_p) and in the interior of the greenhouse (k_i).

Date	k_p	k_i	k_{i-max}	k_{i-min}
22/07/2008	-	0.007	0.016	0.02
11/08/2008	0.05	0.012	0.021	0.06

Energy levels

On the whole, in the empty greenhouse the levels of kinetic energy inside the greenhouse were greater than in the greenhouse with the crop (Table 5). For the two tests analyzed, the air entering the greenhouse through the evaporative pad (*Points 1*) presents much lower levels of turbulent kinetic energy than inside the greenhouse (*Points 2 to 7*). In the presence of a crop, the kinetic energy was greater in the first span closest to the pad (*Points 2*) than at the others points where it fell gradually until reaching the exit (Fig. 11a), whereas without crop the kinetic energy increased gradually and slightly from the pad to the fans (Fig. 11b).

The values of kinetic energy at all points are lower than those recorded in conditions of natural ventilation by Boulard *et al*. (2000) in greenhouses without insect-proof screens, over 10 $m^2 s^{-2}$ on the windward side. Also, Wang and Deltour (1999) recorded values of up to 2.37 $m^2 s^{-2}$ in the interior of the greenhouse.

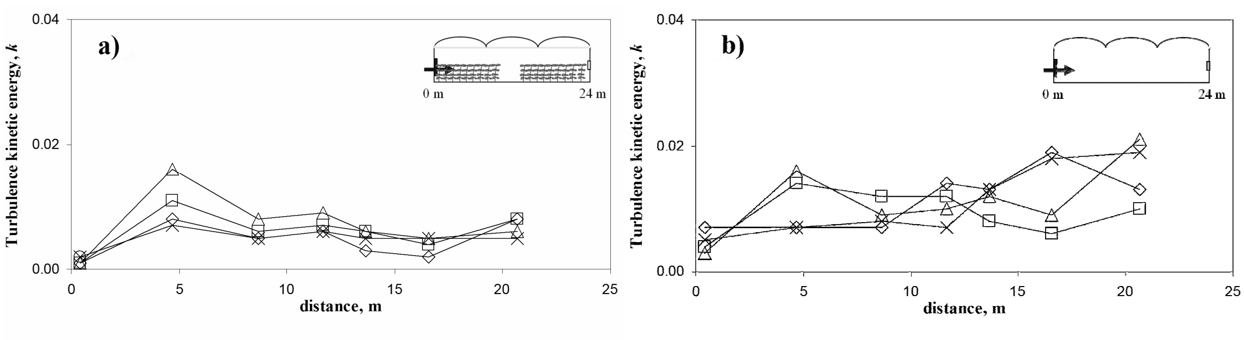

Figure 11. Profiles of turbulent kinetic energy k ($m^2 s^{-2}$) corresponding to the measurement test on 22/07/08 with crop (a) and on 11/08/2008 without crop (b): (-□-)section I; (-Δ-)section II; (-◊-)section III; (-×-)section IV.

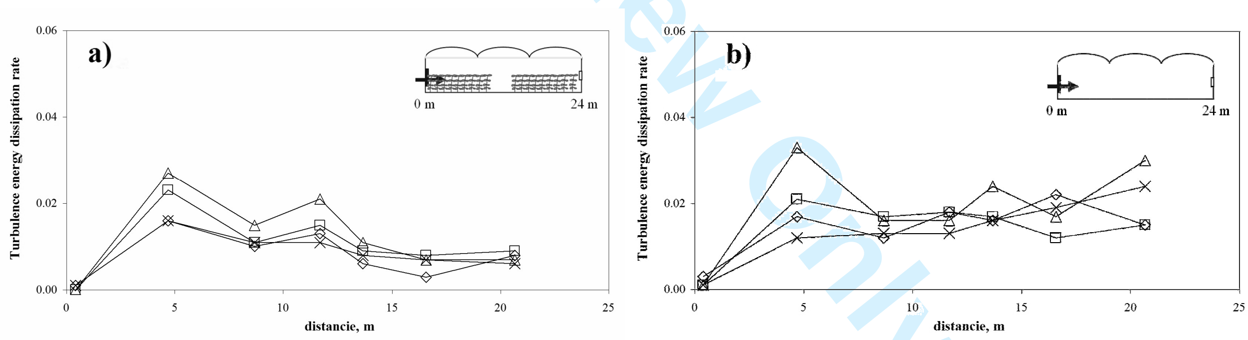

Figure 12. Profiles of Turbulence energy dissipation rate ($m^2 s^{-3}$) corresponding to the measurement test on 22/07/08 with crop (a) and on 11/08/2008 without crop (b): (-□-)section I; (-Δ-)section II; (-◊-)section III; (-×-)section IV.

At the outlet of the evaporative pads, the values of the turbulence energy dissipation rate are practically null (Fig. 12), and the greatest dissipation of energy occurs in the first span (where the air mixes more) in the greenhouse with crop. The evolution of the turbulence energy dissipation rate inside the greenhouse (Fig. 12) shows a similar evolution to the kinetic energy (Fig. 11). As with the values of ***k***, it can be seen that in conditions of mechanical ventilation the values of the turbulence energy dissipation rate are much lower than those recorded by Boulard *et al.* (2000) in conditions of natural ventilation and in greenhouses without insect-proof screens, over 10 $m^2 s^{-3}$.

INTERIOR MICROCLIMATE

Figure 13a reflects the difference between mean outside temperature during the test ($\boldsymbol{T_e}$) and the mean temperature recorded with the sensors ($\boldsymbol{T_i}$). Figure 13b shows the difference between inside ($\boldsymbol{x_i}$) and outside absolute humidity ($\boldsymbol{x_e}$). The points on the graphs that are not joined by lines correspond to the values recorded at the exit of the pads in both tests. Figure 13a shows that greater temperature drops are recorded when there is a crop in the greenhouse. The system tested does not seem suitable to maintain the favourable conditions that allow crop transplant to be brought forward to early August.

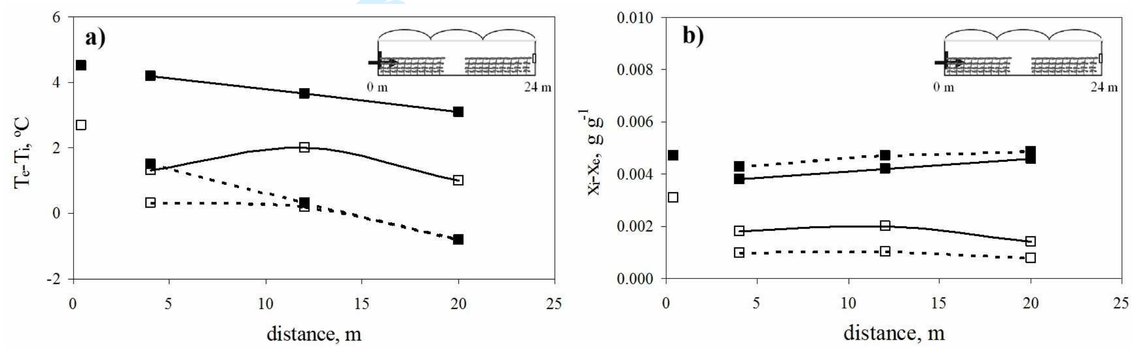

Figure 13. Gradients of temperature (a) between the inside (T_i) and outside (T_e) and gradients of absolute humidity (b) between the inside (x_i) and outside (x_e) of the greenhouse for the measurement test with crop on 22/07/08 (■) and without crop on 11/08/09 (□). The continuous line corresponds to the profile at a height of 1 m, the dotted line at 2 m.

Cooling systems using evaporative pads usually present horizontal and vertical temperature gradients (Kittas *et al.*, 2001). The horizontal temperature gradients recorded inside the greenhouse were 0.07 ºC m^{-1} (1 m above the ground) and 0.27 ºC m^{-1} (2 m above the ground) in the greenhouse with crop; and 0.09 ºC m^{-1} (1 m above the ground) and 0.18 ºC m^{-1} (2 m above the ground) in the empty greenhouse (Fig. 13a). The values recorded at 1 m above the ground were lower than the maximum temperature gradient of 0.13 ºC m^{-1} observed by Kittas *et al.* (2003) in a greenhouse of 60 m length, but the values at 2 m were greater (corresponding to the uppermost part of the crop). Overall, greater temperature drops are achieved in the presence of a crop (Fig. 13a), coinciding with the observations of Willits and Li (2005). The northern sector, where the extractor fans are located, was the least favorable area, and the temperature here even surpassed that outside the greenhouse on 22/07/2008 and 11/08/2008.

The vertical gradients increased with the distance from the pad, and they were higher in the presence of the crop (ranging from 2.7 ºC m^{-1} at a distance of 4 m from the pad to 3.9 ºC m^{-1} at 20 m) than in the empty greenhouse (ranging from 1.0 ºC m^{-1} at 4 m from the pad to 1.8 ºC m^{-1} at 20 m). However, the horizontal and vertical temperature gradients were higher inside the greenhouse with plants than in the empty one, the temperature difference between inside and outside was always greater for the greenhouse with crop. Overall the temperature gradients were greater in the vertical plane than in the horizontal one.

In the presence of the crop, greater increases were observed the humidity of the air along all the transversal cross-section of the greenhouse. The evapotranspiration of the crop increased the water content of the inside air, which is transported by the air flow. Thus, with crop, the air humidity increases with height and with distance from the evaporative pads (Fig 13b). In the measurement without crop it has been observed that the air accumulates greater water content in the lower zone of the greenhouse and closer to the evaporative pads (Fig. 13b).

This climate heterogeneity could be a consequence of the low level of air flow turbulence, a common feature of mechanically generated ventilation. The temperature and humidity gradients are the main disadvantage of the pad-fan cooling system (Arbel et al., 2003; Kittas et al., 2003), as they can lead to over-consumption of irrigation water or nitrogen loss to the environment (Boulard and Wang, 2002).

The average efficiency of the evaporative pad, calculated from the average air temperature at a distance of 40 cm from the pad, was 81.5% over the two measurement tests, with and without crop, coinciding furthermore with the value obtained by Kittas *et al*. (2001).

Horizontal distribution of temperature inside the greenhouse

As well as the temperature measurements by the fixed sensors, a horizontal distribution of temperatures was obtained at a height of 1.5 meters by means of sonic anemometry corrected for inside humidity.

In order to compare the values of temperature measured at different moments in time, we have studied the difference between sonic anemometry at each instant and average instantaneous greenhouse temperature. During the test with crop the mean inside temperature was 27.9 ºC (26.3 ºC average value at a height of 1 m and 29.6 ºC at 2 m) while the mean outside temperature was 29.9 ºC. When the greenhouse was empty these values were 27.9 ºC (26.3 ºC at a height of 1 m and 28.7 ºC at 2 m), while the outside temperature was 28.6 ºC.

In Figure 14 the temperature distribution inside the greenhouse is seen to be more uniform in the presence of the crop. The difference in temperature between the coldest area close to the pads and the warmest area at the extractor fans was 2.3 ºC in the measurements on 11/07/2008 (Fig. 14a). Without crop this difference was greater, 4.0 ºC in the measurements on 11/8/2008 (Fig. 14b).

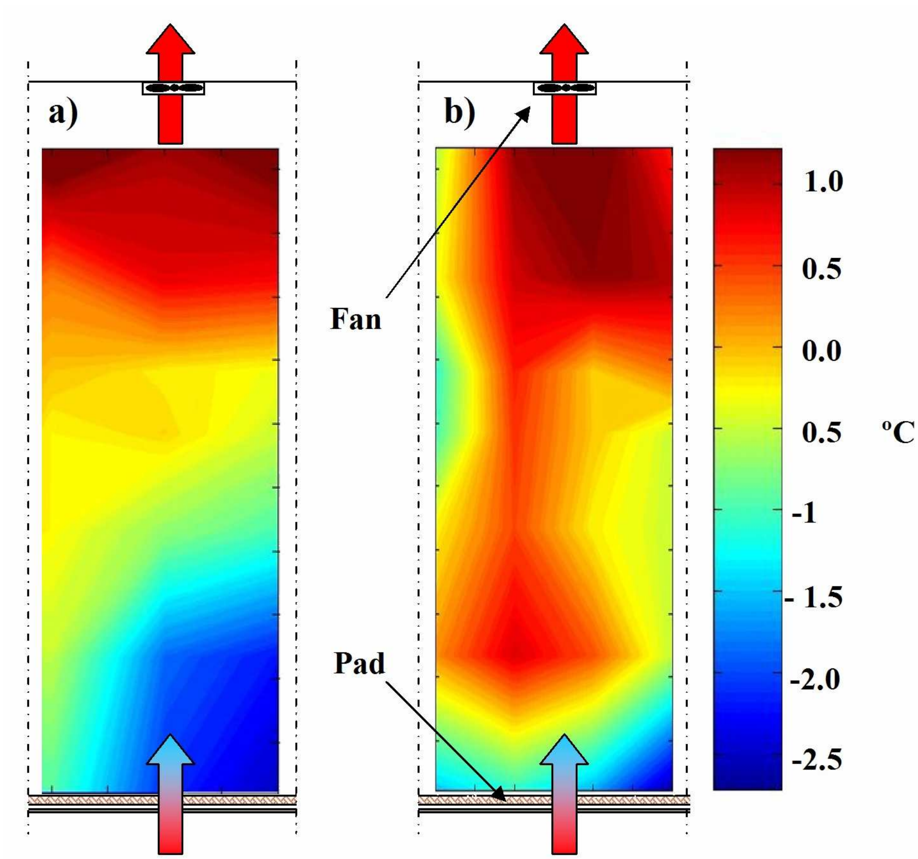

Figure 14. Horizontal distribution of difference between corrected sonic temperature and average instantaneous greenhouse temperature. Measurement test on 22/07/08 with crop (a) and without crop on 11/08/09 (b).

It can be seen that in much of the greenhouse without crop the temperature is even higher than outside, which would make it difficult to bring forward transplant to early August in the Mediterranean region. The fan-pad system forces the outside air into the greenhouse through a wet pad, which humidifies and cools it only at the entrance, where the wet pad is situated. Sethi and Sharma (2007) concluded that this system is not able to treat the accumulated excessive heat (absorbed solar energy) in the greenhouse, as we can also observe from the horizontal temperature distribution measured with the sonic anemometer.

CONCLUSIONS

The air flow generated by mechanical ventilation follows the direction perpendicular to the evaporative pads, and the transversal and vertical components play a less important role. This effect on the air flow direction increases when a crop is present. In this case the air velocity is influenced by the separation between the rows of crop. Also, a predominant direction of the air eddies is created for the horizontal component $\boldsymbol{u_x}$, perpendicular to the pads. In this direction the macroscale is maximum, while in the transversal and vertical directions it is practically null.

When the cool damp air form the pad comes into contact with the mass of warm dry air inside the greenhouse, the air velocity falls, which brings about a sharp increase in the turbulence of the air flow (turbulence intensity, turbulence kinetic energy, turbulence kinetic energy dissipation rate and slope of the spectrum of energy density). This increase in turbulence was less in the presence of the crop, which indicates the crop has a dispersion effect on the air momentum, which is characteristic of porous media.

On the whole, the levels of turbulence (turbulence intensity, kinetic turbulent energy and its dissipation rate) measured inside the experimental greenhouse operating with a fan-pad cooling system were lower than the values observed in naturally ventilated greenhouses reported in the literature. This lower turbulence of the air flow reduces the mixing of the outside air entering the greenhouse through the evaporative pad with the inside air, and contributes to the climate heterogeneity that is the main disadvantage of the pad-fan cooling system. When young plants are transplanted in the greenhouse, this heterogeneity may produce over-consumption of irrigation water, which must be considered by growers to avoid plant damage by water stress.

The system of evaporative pads was less effective when there was no crop, as there was lower temperature reduction with respect to the outside climatic conditions. When plants are transplanted at the end of summer, which is when there is greatest need to reduce temperatures and increase humidity in regions with a high concentration of greenhouses such as Almería (Spain), evaporative pad cooling systems should be devised in order to reduce the temperature gradient.

In the currently available commercial climate controllers there is usually only one temperature and humidity measurement point in the central area of the greenhouse. We recommend studying the ideal number of points and their location in each specific installation, in order that climate control should take into account the most favorable and unfavorable zones. This is particularly important in commercial greenhouses which have a much greater surface area than the experimental greenhouse in the present study, and in which greater temperature gradients are to be expected.

ACKNOWLEDGEMENTS

The authors wish to express their gratitude to the Spanish Ministerio de Educación y Ciencia for partially financing the present work by means of the research grants AGL2006-09068/AGR and BIA2006-12323.

REFERENCES

ANSI/ASAE EP406.1. 1994. Heating, Ventilating and Cooling Greenhouses. St. Joseph, Mich.: ASABE.

ANSI/ASAE EP406.4 JAN03 (R2008). 2003. Heating, Ventilating and Cooling Greenhouses. St. Joseph, Mich.: ASABE.

Arbel, A., M. Barak and A. Shklyar. 2003. Combination of Forced Ventilation and Fogging Systems for Cooling. Greenhouses. Biosystems Eng. 84(1): 45-55.

ASHRAE. 1983. ASHRAE Evaporative air cooling equipment, Equipment Handbook. Atlanta, Ga.: ASHRAE.

Boulard, T., J.F. Meneses, M. Mermier and G. Papadakis 1996. The mechanisms involved in the natural ventilation of greenhouses. Agric. For. Meteorol. 79: 61-77.

Boulard, T. and S. Wang, 2002. Experimental and numerical studies on the heterogeneity of crop transpiration in plastic tunnel. Comput. Electron. Agric. 34: 173–190.

Boulard, T., C. Kittas, G. Papadakis and M. Mermier 1998. Pressure Field and Airflow at the Opening of a Naturally Ventilated Greenhouse. J. agric. Engng Res. 71: 93-102.

Boulard, T., S.Wang and R. Haxaire. 2000. Mean and turbulent air flows and microclimatic patterns in an empty greenhouse tunnel. Agric. For. Meteorol. 100: 169-181.

Capel, J.J. 1990. Climatología de Almería. Cuadernos monográficos 7. Instituto de Estudios Almerienses. Diputación Provincial de Almería (Spain).

Castilla, N. and J. Hernández. 2005. The plastic greenhouse industry of Spain. Chron. Hort. 45 (3): 15-20.

Cebeci, T. 2004. Analysis of Turbulent Flows. California State University, USA: Elsevier Science.

Chung, T.J. 2002. Computational Fluid Dynamics. Cambridge (United Kingdom): Cambridge University Press.

Cuerva, A. and A. Sanz-Andrés. 2000. On sonic anemometer measurement theory. J. Wind Eng. Ind. Aerodyn. 88: 25-55.

Easom, G. 2000. Improved turbulence models for computational wind engineering. MS thesis, Nottingham, United Kingdom: University of Nottingham, School of Civil Engineering.

Fang, F. 1997. A design method for contractions with square end sections. Transactions of the ASME. 119: 454-458.

Fang, F., J.C. Chen, and Y.T. Hong. 2001. Experimental and analytical evaluation of flow in a square-to-square wind tunnel contraction. J. Wind Eng. Ind. Aerodyn. 89: 247-262.

Hazawa, H., A.K. Melikov and P.O. Fanger. 1987. Airflow characteristics in the occupied space. ASHRAE Transactions. 93(1): 524-539.

Heber, A.J. and C.R. Boon. 1993. Air velocity characteristics in an experimental livestock building with non-isothermal jet ventilation. ASHRAE Trans. Symposia. 99 (1): 1139-1151.

Heber, A.J., C.R. Boon and M.W. Peugh. 1996. Air patterns and turbulence in an experimental livestock building. J. Agric. Engng Res. 64: 209-226.

Hellickson, M.A. and J.N. Walker. 1983. Ventilation of Agricultural Structures. ASAE Monograph nº 6. St. Joseph, Mich.: ASABE.

Hinze, J.O. 1975. Turbulence. New York, USA: McGraw-Hill.

Kittas, C., T. Bartzanas and A. Jaffrin. 2001. Greenhouse evaporative cooling: measurement and data analysis. Transactions of the ASAE. 44(3): 683-689.

Kittas, C., T. Bartzanas and A. Jaffrin. 2003. Temperature gradients in a partially shaded large greenhouse equipped with evaporative cooling pads. Biosystems Eng. 85 (1): 87-94.

Lathi, B.P. 1994. Introducción a la teoría y sistemas de comunicación. Balderas, México: Ed. Limusa.

Lay, R.M. and G.M. Bragg. 1988. Distribution of Ventilation Air - Measurement and Spectral Analysis by Microcomputer. Building and Environment. 23(3): 203-213.

Li, S. and D.H. Willits. 2008. An experimental evaluation of thermal stratification in a fan-ventilated greenhouse. Transactions of the ASABE. 51(4): 1443-1448.

Loomans, M.G.L.C. 1998. The measurement and simulation of indoor airflow. MS thesis, Eindhoven, The Netherlands: Technische Universiteit Eindhoven.

Mathieu, J. and J. Scott, 2000. An introduction to turbulent flow. Cambridge, United Kingdom: Cambridge University Press.

Melikov, A.K., G. Langkilde and B. Derbiszewski. 1990. Airflow characteristic in the occupied zone of rooms with displacement ventilation. ASHRAE Transactions. 96 (1): 555-563.

Molina-Aiz, F.D., D.L. Valera, D.L., A.J. Álvarez and A. Madueño. 2006. A Wind Tunnel Study of Airflow through Horticultural Crops: Determination of the Drag Coefficient. Biosystems Eng. 93: 447-457.

Molina-Aiz, F.D., D.L. Valera, A.A. Peña, J.A. Gil, and A. López. 2009. A Study of Natural Ventilation in an Almería-Type Greenhouse with Insect Screens by Means of Tri-sonic Anemometry. Biosystems Eng. 104: 224-242.

Panofsky, H. A., and J.A. Dutton. 1984. Atmospheric Turbulence: Models and Methods for Engineering Applications. New York. USA: Ed. John Wiley and Sons.

Pope S.B. 2009. Turbulent flows. Cambridge, United Kingdom: Cambridge University Press.

Ouyang, Q., W. Dai, H. Li and Y. Zhu., 2006. Study on dynamic characteristics of natural and mechanical wind in built environment using spectral analysis. Building and Environment. 41: 418-426.

Sethi V.P. and S.K. Sharma. 2007. Survey of cooling technologies for worldwide agricultural greenhouse applications. Solar Energy. 81: 1447-1459.

Shilo, E., M. Teitel, Y. Mahrer and T. Boulard. 2004. Air-flow patterns and heat fluxes in roof-ventilated multi-span greenhouse with insect-proof screens. Agric. For. Meteorol. 122: 3-20.

Stull, R.B., 1988. An Introduction to Boundary Layer Meteorology. Dordrecht, The Netherlands. Kluwer Academics Publishers.

Tanny, J., L. Haijun and S. Cohen. 2006. Airflow characteristics, energy balance and eddy covariance measurements in a banana screenhouse. Agricultural and Forest Meteorology. 139 (1-2): 105–118.

Tanny, J., V. Haslavsky and M. Teitel. 2008. Airflow and heat flux through the vertical opening of buoyancy-induced naturally ventilated enclosures. Energy and Buildings. 40: 637-646

Teitel, M., J. Tanny, D. Ben-Yakir and M. Barak. 2005. Airflow Patterns through Roof Openings of a Naturally Ventilated Greenhouse and their Effect on Insect Penetration. Biosystems Eng. 92(3): 341-353.

Teitel, M., O. Liran, J. Tanny and M. Barak. 2008. Wind driven ventilation of a mono-span greenhouse with a rose crop and continuous screened side vents and its effect on flow patterns and microclimate. Biosystems Engineering. 101 (1): 111–122.

Valera, D. L., A.J. Álvarez and F.D. Molina. 2006. Aerodynamic analysis of several insect-proof screens used in greenhouses. Span. J. Agric. Res. 4(4): 273-279.

Valera, D. L., F.D. Molina and A. J. Álvarez 2008. Ahorro y eficiencia energética en invernaderos. Madrid, Spain: Ministerio de Industria, Turismo y Comercio. IDAE.

Valera, D.L., A. López, F.D. Molina-Aiz and A.J. Álvarez. 2009. Estudio del flujo de aire y de la turbulencia en las aperturas de ventilación en invernaderos mediterráneos. In V Congreso Nacional y II Congreso Ibérico de Agroingenería. Departamento de Ingeniería Agroforestal. E.P.S. Campus Universitario. Lugo, Spain.

Wang, S., and J. Deltour. 1997. Natural ventilation induced airflow patters measured by an ultrasonic anemometer in Venlo-type greenhouse openings. Agric. Engng J. 6: 185–196.

Wang, S,. and J. Deltour. 1999. Lee-side ventilation-induced air movement in a large-scale multi-span greenhouse. J. Agric. Engng Res . 74: 103–110.

Wang, S., M. Yernaux and J. Deltour. 1999. A Networked Two-Dimensional Sonic Anemometer System for the Measurement of Air Velocity in Greenhouses. J. Agric. Engng Res. 73: 189-197.

Willits, D.H., and M.M. Peet. 2000. Intermittent application of water to an externally mounted, greenhouse shade cloth to modify cooling performance. Transactions of the ASAE. 43(5): 1247-1252.

Willits, D.H., and S. Li. 2005. A Comparison of Naturally Ventilated vs. Fan Ventilated Greenhouses in the Southeastern U.S. ASAE Annual International Meeting. Florida (USA).

Wittwer, S.H. and N. Castilla. 1995. Protected cultivation of horticultural crops worldwide. HorTechnology. 3: 6-19.

NOMENCLATURE

D	wind direction (º)
E	spectral density ($m^2 s^{-1}$)
HR	relative humidity (%)
L_i	integral length scale (m)
NE	northeast
R	normalized autocorrelation function ($m^2 s^{-2}$)
SW	southwest
T	temperature (ºC)
$X(f)$	the Fast Fourier Transfer (FFT) of sample data

$X^*(f)$	conjugate complex number of X
$X(t)$	sample data
f	frecuency (Hz)
i	turbulence intensity
k	turbulence kinetic energy ($m^2\ s^{-2}$)
l	two-dimensional horizontal resultant of air velocity in XY plane ($m\ s^{-1}$)
q	specific humidity of the air ($g\ g^{-1}$)
t	time (s)
t_0	first zero crossing of normalized autocorrelation function
t_{int}	integral time scale (s)
Δt	time interval
u	air velocity ($m\ s^{-1}$)
$\bar{u}$	time-mean value of air velocity ($m\ s^{-1}$)
u'	fluctuating component ($m\ s^{-1}$)
$\bar{u}_{ext}$	mean wind velocity
v	two-dimensional vertical resultant of air velocity in XZ plane ($m\ s^{-1}$)
x	absolute humidity of air ($g\ g^{-1}$)

GREEK LETTERS

σ	standard deviation ($m\ s^{-1}$)
δ_t	time (s)
ε	turbulence energy dissipation rate ($m^2\ s^{-3}$)
λ	microescale (m)
β	power spectrum exponent
η	cooling efficienency (%)

SUBSCRIPTS

bh	wet bulb of the outside air
bs	dry bulb of the outside air
cbs	dry bulb of the air leaving the pad

e	outside
i	inside
max	maximum
min	minimum
p	pad
s	sonic
sc	sonic corrected
x	longitudinal component
y	transversal component
z	vertical component